

## Research Article

# Preparation of Polyamide 6/CeO<sub>2</sub> Composite Nanofibers through Electrospinning for Biomedical Applications

Xinyu Zhang <sup>1</sup> and Xinggang Chen <sup>2</sup>

<sup>1</sup>College of Fashion and Design, Donghua University, Shanghai, China

<sup>2</sup>College of Material Science and Engineering, North China University of Science and Technology, Tangshan, China

Correspondence should be addressed to Xinggang Chen; [chenxinggang000@126.com](mailto:chenxinggang000@126.com)

Received 18 July 2019; Revised 19 November 2019; Accepted 25 November 2019; Published 11 December 2019

Academic Editor: Domenico Acierno

Copyright © 2019 Xinyu Zhang and Xinggang Chen. This is an open access article distributed under the Creative Commons Attribution License, which permits unrestricted use, distribution, and reproduction in any medium, provided the original work is properly cited.

Polyamide 6 (PA6)/CeO<sub>2</sub> composite nanofibers were prepared by electrospinning technique. The morphological, structural, and mechanical properties of the PA6/CeO<sub>2</sub> nanofibers were investigated by using SEM, XRD, Fourier transform-infrared (FT-IR) spectroscopy, and an electronic universal tensile testing machine. SEM images revealed that the nanofibers were well oriented and had good incorporation with CeO<sub>2</sub>, the average diameter of composite fibers first decreases and then increases with the loading of CeO<sub>2</sub>. The crystallinity of fibers decreases after the addition of CeO<sub>2</sub>. The tensile strength of the fibers first increases and then decreases with the increasing concentration of CeO<sub>2</sub>. The proliferation properties of mouse macrophages and osteoblasts on the PA6/CeO<sub>2</sub> nanofibers were analyzed by an in vitro cell compatibility test, the results show that PA6/CeO<sub>2</sub> composite fibers is nontoxic to macrophages and osteoblasts and has good biocompatibility.

## 1. Introduction

As a biodegradable, biocompatible, and synthetic polymeric kind of material, polyamide 6 (PA6) has good mechanical and physical properties, is nontoxic, and has wear resistance [1, 2]. Due its chemical structure, and since the reactive group is similar to collagen, PA6 is also widely used as a biological material, such as surgical sutures, artificial blood vessels, artificial muscles, and artificial bone. However, as for biomedical materials, although PA6's comprehensive properties have been relatively perfect, it needs further surface modification to increase the multifunctional applications [3, 4].

Electrospinning is an efficient technique to fabricate continuous fibers with high surface area-to-volume ratio and high porosity [5, 6]. The high application potential of electrospinning to biological polymers has increased since the electrospun membranes were regarded as a candidate for tissue engineering constructs [7, 8]. PA6 and its composites could also be prepared or has increased multifunctional applications as nanoscale materials by electrostatic

spinning under suitable conditions, when dissolved in highly polar solvent, such as formic acid [9, 10]. Abdalhay et al. [11] found that the average diameters of HAp/PA6 fibers firstly decreased and then increased with the increase of HAp content. Ahn et al. [4] observed that the concentration of PA6 solution had an important effect on the nanostructure of ES products. Pant et al. [12] observed that standing time could influence the diameter of Ag/PA6 nanofibers in the pretreatment of blend solution of AgNO<sub>3</sub>/PA6. Nirmala et al. [13, 14] investigated PA6/chitosan composite nanofibers that were successfully prepared via electrospinning with diameters of about 20 to 40 nm. In a word, it can be seen that from the above analyses, the functional properties of PA nanofibers can be improved by adding crosslinking agents like HAp, Ag, and chitosan. However, since the biological activity of PA6 is insufficient, new bioactive nanoparticles need to be further explored to increase the biological activity and other multifunctional applications of PA nanofibers.

Cerium oxide (CeO<sub>2</sub>), a rare earth metal oxide of the lanthanide series, has a face centered cubic fluorite-type crystal

structure and exists in two oxidation states +3 and +4 [15, 16]. The  $Ce^{3+}/Ce^{4+}$  redox switch and oxygen vacancies by surface defects make the  $CeO_2$  nanoparticles have redox and biological activities, and can promote the growth and differentiation of osteoblasts, and improve the biological activity and antioxidant and anti-inflammatory ability of the biological materials [17–19]. Gojova et al. [20] when studying the effect of metal particles on inflammatory response of vascular endothelial cells found that cerium dioxide has a certain anti-inflammatory ability. Hirst [21] found that cerium dioxide has good biocompatibility and can inhibit inflammatory response by scavenging free radicals and reactive oxygen species. However, with the nanoization of  $CeO_2$ , it also has its own defects. On one hand, the smaller is the particle size of  $CeO_2$ , the more atoms on the surface, leading to the higher surface energy and the easier to form aggregates. On the other hand, as a kind of a biological material, the biological safety of  $CeO_2$  nanomaterials has also gradually attracted our attention.

In this paper, we considered combining PA6 and  $CeO_2$  with electrospinning in order to obtain biomedical nanofibers, which would be used as biological materials, such as surgical sutures, artificial blood vessels, artificial muscles, and artificial bone. Recent papers have already reported on the modification of the functional properties of PA nanofibers; here,  $CeO_2$  nanomaterials are used to improve the biological activity, such as to promote the growth and differentiation of osteoblasts. In what follows, PA6/ $CeO_2$  biomedical composite materials are prepared by combining PA6 with modified nano- $CeO_2$  via electrospinning, the comprehensive properties of composite materials are explored, and the biological safety of nano- $CeO_2$  on composite materials is also investigated. Moreover, we systematically characterized the content of  $CeO_2$  on the diameter, crystallinity and mechanical properties, and cell proliferation of PA/ $CeO_2$  composite fibers. It is expected to provide theoretical and experimental basis for the practical application of PA6/ $CeO_2$  biomedical composites.

**1.1. Experimental.** Granules of PA6, purchased from Dongguan Qiyuan Plastic Material Co., Ltd., China, and the modifying agent  $CeO_2$  were used to prepare the spinning solution. Among them, the modified  $CeO_2$  was obtained by coprocessing with  $CeO_2$  (purchased from Leshan Wolaixi Electronic Materials Co., Ltd., China), KH550 coupling reagent, and absolute ethyl alcohol. PA6 with different concentrations of modified  $CeO_2$  with 0, 3, 5, 7, and 9 wt.% were used to prepare the composite nanofibers. A single solvent, formic acid (analytical grade, Tianjin Yongda Chemical Reagent Co. Ltd., China) was used to prepare the polymer solution. PA6/ $CeO_2$  nanofibers were electrospun in 80% formic acid. A high-voltage power supply of 20 kV was supplied to the syringe microtip to electrospin the nanofibers. The tip-to-collector distance was kept at 18 cm. Polymer solution was placed to the 5 mL syringe with a plastic microtip. Finally, the PA6/ $CeO_2$  nanofibers were vacuum dried at 80°C for 24 h to remove the residual solvent, and then, the nanofibers were used for further characterizations.

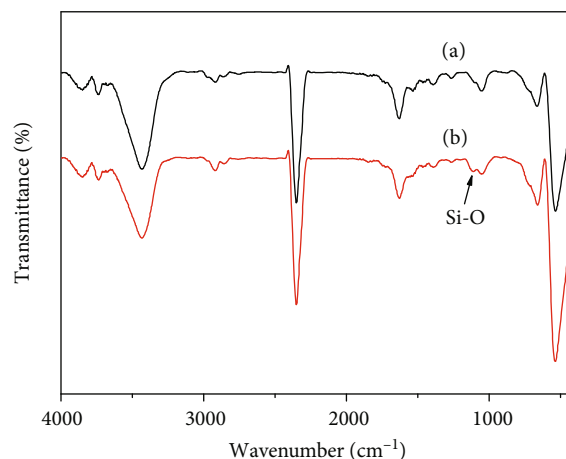


FIGURE 1: FT-IR spectroscopy of (a) unmodified  $CeO_2$  and (b) modified  $CeO_2$  with coupling agent KH550.

The morphology of the PA6/ $CeO_2$  nanofibers was observed by using field-emission scanning electron microscopy (FESEM, S-4800, Hitachi, Japan). Then, the diameters of composite fibers from the SEM images were calculated by a statistics software. The phase composition of electrospun textile sheets (1 cm × 1 cm) has been analyzed by X-ray diffraction (XRD, D/MAX 2500, Rigaku, Japan). The bonding configurations of the nanofibers and modification effect were characterized by means of Fourier transform-infrared (FT-IR, VERTEX 70, Bruker, Germany) and EDS analysis. Tensile strength characterizations were performed for the electrospun PA6/ $CeO_2$  nanofibers by electronic universal tensile testing machine (AGS-X, Shimadzu, Japan) to measure the strength of the fibers under external force.

The cell proliferation effect of  $CeO_2$  on PA6/ $CeO_2$  nanofiber membrane was tested by mouse macrophages and osteoblasts. In order to observe the manner of cell attachment on composite nanofibers, chemical fixation of cells was carried out in PA6 and PA6/5 wt.%  $CeO_2$  samples. After a series of cell culture and incubation, the absorbance value was measured by ELISA, and finally, the samples were prepared for the cell morphology observation by SEM.

## 2. Results and Discussion

**2.1. FT-IR Spectroscopy of PA6/ $CeO_2$  Composite Fibers.** FT-IR spectroscopy was used to study the changes of the functional groups of modified  $CeO_2$  with coupling agent KH550 and unmodified  $CeO_2$ , as shown in Figure 1.

It can be seen that the wide peak around 3400  $cm^{-1}$  is the absorption peak generated by the stretching vibration of water molecules. Moreover, the absorption peak of Si-O and C-H bonds appear at 1118 and 2923  $cm^{-1}$ , respectively, in Figure 1(b) in the modified  $CeO_2$ . Therefore, it can be proven that the coupling agent KH550 was successfully coated on the surface of nano- $CeO_2$ .

EDS measurement was used to confirm if the coupling agent KH550 coated on the surface of nano- $CeO_2$ , as shown in Figure 2. It can be seen from Figure 2(b) that the small

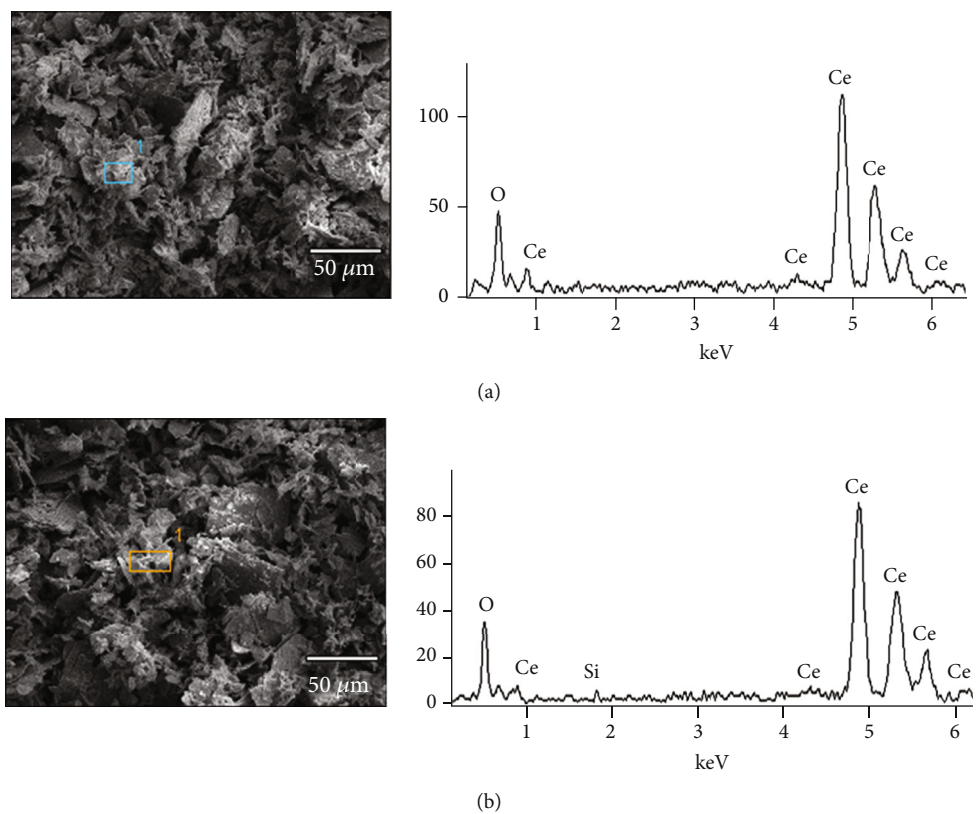


FIGURE 2: SEM and EDS diagrams of (a) unmodified  $\text{CeO}_2$  and (b) modified  $\text{CeO}_2$  with coupling agent KH550.

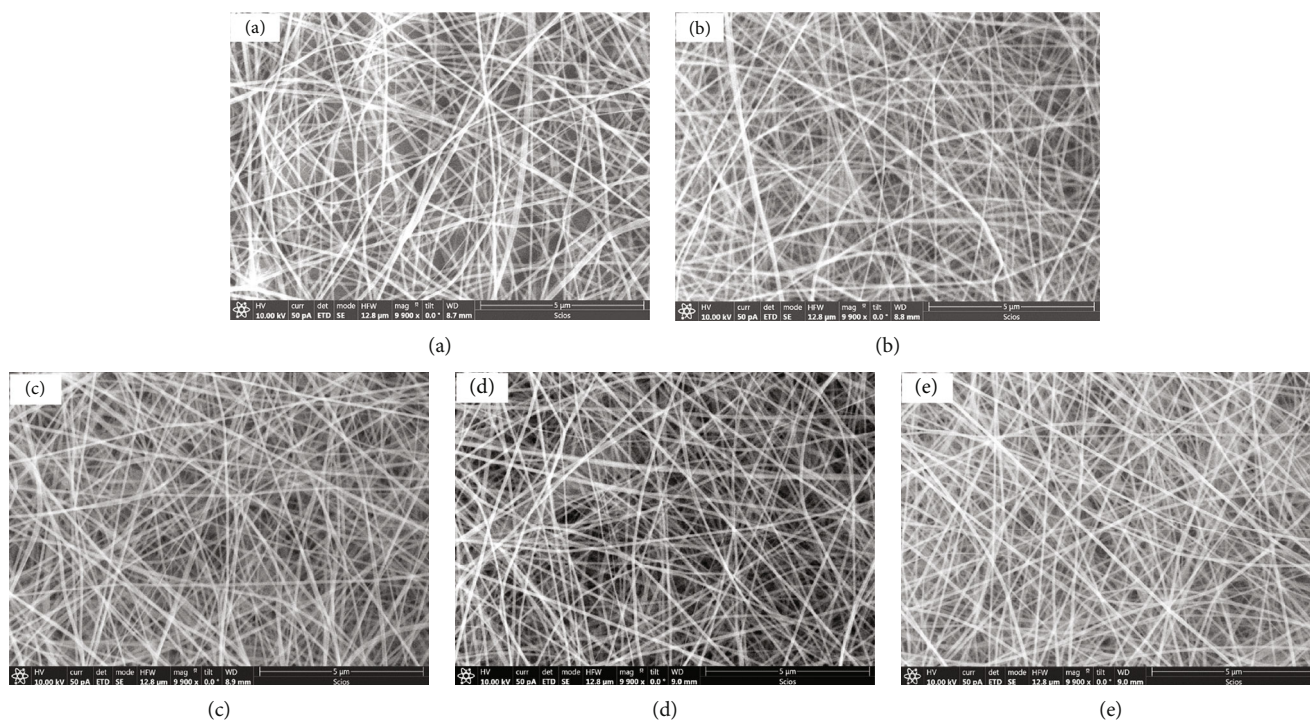
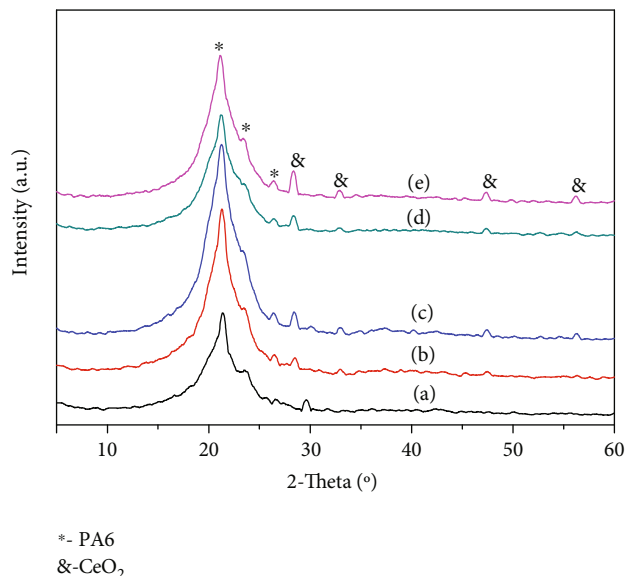


FIGURE 3: SEM images of composite fibers with the different concentrations of  $\text{CeO}_2$ : (a) 0 wt.%, (b) 3 wt.%, (c) 5 wt.%, (d) 7 wt.%, and (e) 9 wt.%.

TABLE 1: The diameter of composite fibers with the different CeO<sub>2</sub> concentrations.

Fibers samples	0 wt.% CeO <sub>2</sub>	3 wt.% CeO <sub>2</sub>	5 wt.% CeO <sub>2</sub>	7 wt.% CeO <sub>2</sub>	9 wt.% CeO <sub>2</sub>
Average diameter (nm)	430	400	370	410	450
Standard deviation	11.0	11.99	8.69	16.1	17.2
Maximum (nm)	640	700	520	720	760
Minimum (nm)	280	190	160	180	160

FIGURE 4: XRD patterns of PA6/CeO<sub>2</sub> composite fibers with the different concentrations of CeO<sub>2</sub>: (a) 0 wt.%, (b) 3 wt.%, (c) 5 wt.%, (d) 7 wt.%, and (e) 9 wt.%.

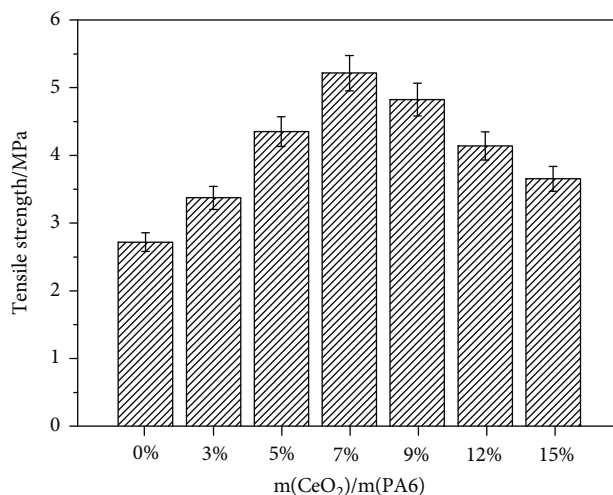
peak appearing at around 1.85 KeV is a characteristic peak of the Si element in the silane coupling agent, so it can also be proven that the KH550 coupling agent is successfully grafted on the surface of the nano-CeO<sub>2</sub>, while the rate is limited.

**2.2. Morphology of PA6/CeO<sub>2</sub> Composite Fibers.** The effect of modified CeO<sub>2</sub> on PA6 nanofiber is investigated, and Figures 3(a)–3(e) show the SEM images of electrospun PA6/CeO<sub>2</sub> nanofibers for the different concentrations of modified CeO<sub>2</sub> with 0, 3, 5, 7, and 9 wt.%, respectively. The electrospun fibers in Figures 3(a)–3(e) all exhibit a smooth surface and uniform diameters along their lengths, and there are no obvious difference with the change of CeO<sub>2</sub> concentration. Then, the diameters of composite fibers from the SEM photos were calculated by a statistics software, as shown in Table 1. It shows that the average diameter of composite fibers first decreases and then increases with the increase of CeO<sub>2</sub> content, reaching the minimum value of 370 nm when the content of CeO<sub>2</sub> is 5 wt.%.

The reason for this phenomenon may be that when the content of CeO<sub>2</sub> increases from 0 wt.% to 5 wt.%, the concentration of solution increases and the charge density on the jet surface increases, leading to more charges on the jet, thus increasing the tensile force and decreasing the diameter of the fiber. However, when the content of CeO<sub>2</sub> increased from

TABLE 2: Crystallinity of PA6/CeO<sub>2</sub> composite fibers with the different concentrations of CeO<sub>2</sub>.

Fibers samples	Crystallinity
0 wt.% CeO <sub>2</sub>	58.48%
3 wt.% CeO <sub>2</sub>	52.07%
5 wt.% CeO <sub>2</sub>	47.42%
7 wt.% CeO <sub>2</sub>	45.77%
9 wt.% CeO <sub>2</sub>	41.91%

FIGURE 5: Tensile properties of PA6/CeO<sub>2</sub> composite fibers with the different concentrations of CeO<sub>2</sub>.

7 wt.% to 9 wt.%, the diameter of composite fibers increased. It may be that the viscosity is too high, which makes the fibers entangled with each other, leading to a decrease in splitting ability and an increase in diameter. Thus, when the content of CeO<sub>2</sub> is 5 wt.%, the fiber diameter is the minimum, and the change of fiber diameter is also the smallest.

**2.3. The Crystallinity of PA6/CeO<sub>2</sub> Composite Fibers.** In order to investigate the effect of the concentration of CeO<sub>2</sub> on the crystalline structures of PA6, the PA6/CeO<sub>2</sub> composite fiber film was studied by XRD, and the result is shown in Figure 4. The diffraction pattern of PA6 nanofibers exhibited a broad peak which appeared at  $2\theta = 21.42^\circ$  and two weak peaks at  $23.53^\circ$  and  $26.37^\circ$  corresponding to the characteristic of the PA6. However, the XRD data of PA6/CeO<sub>2</sub> nanofibers were a little weak to provide a significant result, only several weak characteristic peaks of CeO<sub>2</sub> appeared at  $28.29^\circ$ ,  $32.87^\circ$ ,  $47.26^\circ$ , and  $56.34^\circ$ . In addition, the crystallinity of composite fibers with different CeO<sub>2</sub> concentrations is listed in Table 2.

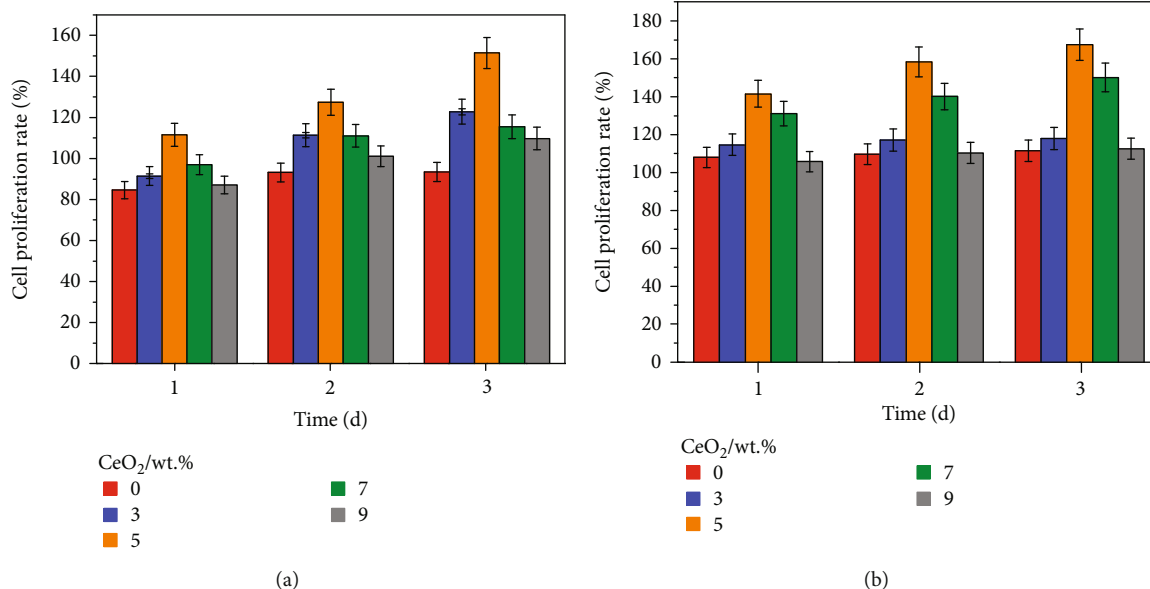


FIGURE 6: Cell growth measurement on (a) macrophages and (b) osteoblasts of electrospun PA6/CeO<sub>2</sub> nanofibers with CeO<sub>2</sub> concentrations of 0 wt.%, 3 wt.%, 5 wt.%, 7 wt.%, and 9 wt.%.

As can be seen from Table 2, the crystallinity of composite fibers decreases after the addition of CeO<sub>2</sub> and declines continually with the increase of CeO<sub>2</sub> content. When the content of CeO<sub>2</sub> was 9 wt.%, the crystallinity was the lowest, 41.91%. This phenomenon may be due to the agglomeration of nanoparticles that occurs with the excessive content of CeO<sub>2</sub>, which disturbs the regular arrangement of macromolecules and reduces the crystallinity of composite fibers.

**2.4. Tensile Properties of PA6/CeO<sub>2</sub> Composite Fibers.** In order to investigate the effect of CeO<sub>2</sub> content on mechanical properties of PA6/CeO<sub>2</sub> composite fibers, tensile properties were conducted by an electronic universal tensile testing machine. The result is shown in Figure 5.

It can be seen from Figure 5 that the tensile strength of fibers first increases with the increased concentration of CeO<sub>2</sub>. The reason for this phenomenon may be that the modified nano-CeO<sub>2</sub> is conducive to the bonding between inorganic and organic substances, so the tensile strength increases. The tensile strength of PA6 composite fibers with 7 wt.% CeO<sub>2</sub> was the highest, reaching 5.22 MPa, which increased by 91.84% than that of the pure PA6 fibers. However, the tensile strength decreases after too much CeO<sub>2</sub> is added, because excessive nano-CeO<sub>2</sub> would become the stress concentration point in PA6 fibers, and then, the tensile strength would decline, leading to the fracture of fibers easily.

**2.5. The Proliferation of Mouse Macrophages and Osteoblasts on PA6/CeO<sub>2</sub> Composite Fibers.** The effects of CeO<sub>2</sub> content on the proliferation of mouse macrophages and osteoblasts were tested by cell experiments. Figure 6 shows the quantitative cell viability test results.

According to Figure 6, the cellular proliferation gradually increases from 1 day to 3 days, and also, the groups with the addition of CeO<sub>2</sub> was higher than those in the blank group, indicating that PA6/CeO<sub>2</sub> electrospinning fibers with CeO<sub>2</sub>

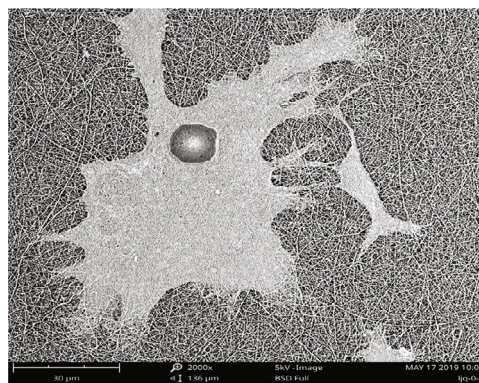


FIGURE 7: SEM image of mouse osteoblast cultured on PA6/5 wt.% CeO<sub>2</sub> composite nanofibers for 1 day.

were non-toxic to macrophages and osteoblasts and has good biocompatibility. Meanwhile, it can also prove that PA6/CeO<sub>2</sub> electrospinning fibers can promote cell proliferation.

Compared with Figures 6(a) and 6(b), it can be seen that the proliferation capacity of CeO<sub>2</sub> for osteoblasts is greater than that of macrophages, and when the content of CeO<sub>2</sub> is 5 wt.%, PA6/CeO<sub>2</sub> electrospinning fibers have the largest ability to promote the proliferation of osteoblasts. By 3 days of culture, the cell proliferation rate reached 167%.

In order to investigate the statistical significance of the cell proliferation effect of cerium oxide, SPSS software was used to analyze the significant difference of the test data in Figure 6, and the results showed that all the PA6/CeO<sub>2</sub> nanofibers from 1 day to 3 days with different CeO<sub>2</sub> concentrations have a significant difference compared with the blank PA6 fiber.

**2.6. Morphology of Mouse Osteoblast on PA6/5 Wt.% CeO<sub>2</sub> Composite Nanofibers.** Figure 7 shows the SEM image of

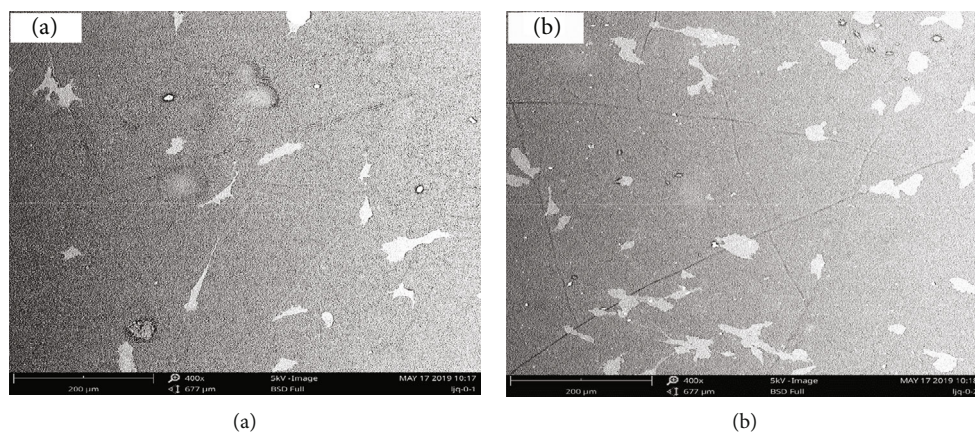


FIGURE 8: SEM images of osteoblasts cultured on (a) pure PA6 fibers, and (b) PA6/5 wt.% CeO<sub>2</sub> composite fiber membrane.

mouse osteoblast cultured on PA6/CeO<sub>2</sub> nanofibers for 1 day. It can be seen that the nucleus of the cell on the fiber membrane is round, which grows along the direction of the fiber on the nanofiber membrane, and it can be clearly seen that the cell has been completely or partially embedded in the fiber interior, and the surface of the membrane is basically completely covered by the cell. Therefore, osteoblasts grow successfully and well in PA6/CeO<sub>2</sub> composite nanofiber membranes.

Figure 8 shows the SEM images of osteoblasts cultured on pure PA6 fibers and PA6/CeO<sub>2</sub> fibers membrane for 1 day. Obviously, the number of cells in the PA6/5 wt.% CeO<sub>2</sub> fiber membrane is significantly higher than that in the pure PA6 fiber membrane. As the scaffold itself, PA6 nanofibers play a role in guiding cell growth, and the number of cells increases significantly after the addition of CeO<sub>2</sub>, so CeO<sub>2</sub> can significantly promote the proliferation of CeO<sub>2</sub> osteoblasts.

### 3. Conclusions

CeO<sub>2</sub> blended in PA6 composite fibers with smooth surface and uniform diameters is successfully prepared by an electrospinning process. High aspect ratio PA6/CeO<sub>2</sub> composite nanofibers with diameters of about 370 to 450 nm were bound in all fibers. It shows that the CeO<sub>2</sub> has no obvious effect on the morphology of PA6 fibers. With the increase of CeO<sub>2</sub> content, the diameter of composite fibers first decreases and then increases, reaching the minimum value of 370 nm at 5 wt.%. The tensile strength of the fibers first increases and then decreases with the increase of CeO<sub>2</sub> content, reaching the best value of 5.22 MPa at 7 wt.%. The crystallinity of PA6 composite fibers decreases after the addition of CeO<sub>2</sub> and declines continually with the increase of CeO<sub>2</sub> content.

PA6/CeO<sub>2</sub> electrospinning membrane is nontoxic to macrophages and osteoblasts and has good biocompatibility. The proliferation capacity of CeO<sub>2</sub> to osteoblasts is greater than that of macrophages, and when the content of CeO<sub>2</sub> is 5 wt.%, PA6/CeO<sub>2</sub> electrospinning fibers have the largest ability to promote the proliferation of osteoblasts. Current results have brought a deeper insight into the formation of

electrospun nanofibers in the presence of a modifying agent CeO<sub>2</sub> and show the pitfalls and benefits in biomedical aspects.

### Data Availability

The data used to support the findings of this study are included within the supplementary information file.

### Conflicts of Interest

The authors declare that they have no conflicts of interest regarding the publication of this paper.

### Acknowledgments

The authors acknowledge the National Science Foundation of China (Grant No. 51874140) and Natural Science Foundation of Hebei Province (Grant No. C2018209270).

### Supplementary Materials

Fig. 1: FT-IR spectroscopy of (a) unmodified CeO<sub>2</sub> and (b) modified CeO<sub>2</sub> with coupling agent KH550. Figure 4: XRD patterns of PA6/CeO<sub>2</sub> composite fibers with the different concentrations of CeO<sub>2</sub>: (a) 0 wt.%, (b) 3 wt.%, (c) 5 wt.%, (d) 7 wt.%, and (e) 9 wt.%. Figure 5: tensile properties of PA6/CeO<sub>2</sub> composite fibers with the different concentrations of CeO<sub>2</sub>. Figure 6: cell growth measurement on (a) macrophages and (b) osteoblasts of electrospun PA6/CeO<sub>2</sub> nanofibers with different CeO<sub>2</sub> concentrations of 0 wt.%, 3 wt.%, 5 wt.%, 7 wt.%, and 9 wt.%. (*Supplementary Materials*)

### References

- [1] S.-Y. Tsou, H.-S. Lin, P.-J. Cheng, C.-L. Huang, J.-Y. Wu, and C. Wang, "Rheological aspect on electrospinning of polyamide 6 solutions," *European Polymer Journal*, vol. 49, no. 11, pp. 3619–3629, 2013.
- [2] P. Heikkilä and A. Harlin, "Parameter study of electrospinning of polyamide-6," *European Polymer Journal*, vol. 44, no. 10, pp. 3067–3079, 2008.

- [3] R. Tripathi, A. Narayan, I. Bramhecha, and J. Sheikh, "Development of multifunctional linen fabric using chitosan film as a template for immobilization of in-situ generated CeO<sub>2</sub> nanoparticles," *International Journal of Biological Macromolecules*, vol. 121, pp. 1154–1159, 2019.
- [4] Y. C. Ahn, S. K. Park, G. T. Kim et al., "Development of high efficiency nanofilters made of nanofibers," *Current Applied Physics*, vol. 6, no. 6, pp. 1030–1035, 2006.
- [5] F. Cui, W. Han, J. Ge, X. Wu, H. Kim, and B. Ding, "Electrospinning: a versatile strategy for mimicking natural creatures," *Composites Communications*, vol. 10, pp. 175–185, 2018.
- [6] N. Bhardwaj and S. C. Kundu, "Electrospinning: a fascinating fiber fabrication technique," *Biotechnology Advances*, vol. 28, no. 3, pp. 325–347, 2010.
- [7] A. Rogina, "Electrospinning process: versatile preparation method for biodegradable and natural polymers and biocomposite systems applied in tissue engineering and drug delivery," *Applied Surface Science*, vol. 296, pp. 221–230, 2014.
- [8] F. E. Ahmed, B. S. Lalia, and R. Hashaikeh, "A review on electrospinning for membrane fabrication: challenges and applications," *Desalination*, vol. 356, pp. 15–30, 2015.
- [9] D. Zhang, D. Liu, Q. Ren, Y. Chen, and C. Yin, "Fabrication of polyamide-6 fiber of high SO<sub>3</sub>H content surface through electrospinning," *Polymer*, vol. 98, pp. 11–19, 2016.
- [10] H. R. Pant, M. P. Bajgai, C. Yi et al., "Effect of successive electrospinning and the strength of hydrogen bond on the morphology of electrospun nylon-6 nanofibers," *Colloids and Surfaces A: Physicochemical and Engineering Aspects*, vol. 370, no. 1-3, pp. 87–94, 2010.
- [11] A. Abdal-hay, H. R. Pant, and J. K. Lim, "Super-hydrophilic electrospun nylon-6/hydroxyapatite membrane for bone tissue engineering," *European Polymer Journal*, vol. 49, no. 6, pp. 1314–1321, 2013.
- [12] B. Pant, H. R. Pant, D. R. Pandeya et al., "Characterization and antibacterial properties of Ag NPs loaded nylon-6 nanocomposite prepared by one-step electrospinning process," *Colloids and Surfaces A: Physicochemical and Engineering Aspects*, vol. 395, pp. 94–99, 2012.
- [13] R. Nirmala, R. Navamathavan, H.-S. Kang, M. H. El-Newehy, and H. Y. Kim, "Preparation of polyamide-6/chitosan composite nanofibers by a single solvent system via electrospinning for biomedical applications," *Colloids and Surfaces B: Biointerfaces*, vol. 83, no. 1, pp. 173–178, 2011.
- [14] R. Nirmala, R. Navamathavan, M. H. El-Newehy, and H. Y. Kim, "Preparation and electrical characterization of polyamide-6/chitosan composite nanofibers via electrospinning," *Materials Letters*, vol. 65, no. 3, pp. 493–496, 2011.
- [15] K. Polychronopoulou and M. A. Jaoudé, "Nano-architectural advancement of CeO<sub>2</sub>-driven catalysis via electrospinning," *Surface and Coatings Technology*, vol. 350, pp. 245–280, 2018.
- [16] D. Noon, B. Zohour, and S. Senkan, "Oxidative coupling of methane with La<sub>2</sub>O<sub>3</sub>-CeO<sub>2</sub> nanofiber fabrics: A reaction engineering study," *Journal of Natural Gas Science and Engineering*, vol. 18, pp. 406–411, 2014.
- [17] M. S. Hassan, R. Khan, T. Amna et al., "The influence of synthesis method on size and toxicity of CeO<sub>2</sub> quantum dots: Potential in the environmental remediation," *Ceramics International*, vol. 42, 1, Part A, pp. 576–582, 2016.
- [18] S. Thanka Rajan, M. Karthika, U. Balaji, A. Muthappan, and B. Subramanian, "Functional finishing of medical fabrics using CeO<sub>2</sub>/allicin nanocomposite for wound dressings," *Journal of Alloys and Compounds*, vol. 695, pp. 747–752, 2017.
- [19] Z. Lu, C. Mao, M. Meng et al., "Fabrication of CeO<sub>2</sub> nanoparticle-modified silk for UV protection and antibacterial applications," *Journal of Colloid and Interface Science*, vol. 435, pp. 8–14, 2014.
- [20] A. Gojova, J.-T. Lee, H. S. Jung, B. Guo, A. I. Barakat, and I. M. Kennedy, "Effect of cerium oxide nanoparticles on inflammation in vascular endothelial cells," *Inhalation Toxicology*, vol. 21, no. sup1, Supplement 1, pp. 123–130, 2009.
- [21] S. M. Hirst, A. S. Karakoti, R. D. Tyler, N. Sriranganathan, S. Seal, and C. M. Reilly, "anti-inflammatory properties of cerium oxide nanoparticles," *Small*, vol. 5, no. 24, pp. 2848–2856, 2009.



**Hindawi**  
Submit your manuscripts at  
[www.hindawi.com](http://www.hindawi.com)

